Research in Astron. Astrophys. **2012** Vol. **12** No. **11**, 1576–1584
http://www.raa-journal.org *http://www.iop.org/journals/raa*

Research in Astronomy and Astrophysics

Possible origin of the Damocloids: the scattered disk or a new region? *

Su Wang[1], Hai-Bin Zhao[1], Jiang-Hui Ji[1], Sheng Jin[1,2], Yan Xia[1], Hao Lu[1], Min Wang[1] and Jin-Sheng Yao[1]

[1] Purple Mountain Observatory, Chinese Academy of Sciences, Nanjing 210008, China; *jijh@pmo.ac.cn*

[2] Graduate University of Chinese Academy of Sciences, Beijing 100049, China

Received 2011 August 30; accepted 2012 April 20

Abstract The Damocloids are a group of unusual asteroids that recently added a new member: 2010 EJ104. The dynamical evolution of the Damocloids may reveal a connection from the Main Belt to the Kuiper Belt and beyond the scattered disk. According to our simulations, two regions may be considered as possible origins of the Damocloids: the scattered disk, or a part of the Oort cloud, which will be perturbed to a transient region located between 700 AU and 1000 AU. Based on their potential origin, the Damocloids can be classified into two types, depending on their semi-major axes, and about 65.5% of the Damocloids are classified into type I which mainly originate from the Oort cloud. Whether the Damocloids are inactive nuclei of the Halley Family of Comets may depend on their origin.

Key words: methods: numerical — celestial mechanics — minor planets, asteroids: Damocloids

1 INTRODUCTION

In our solar system, most asteroids are classified into the following types: I) Main Belt asteroids, near-earth objects, and Jupiter trojans, mostly residing in the inner solar system; II) Centaurs mainly orbiting in the outer solar system between Jupiter and Neptune; III) trans-Neptunian objects located at or beyond the orbit of Neptune, e.g. Neptunian trojans, Kuiper Belt objects and scattered disk objects. Unlike asteroids, there are comets which have visible signs of outgassing in the solar system, such as Jupiter-family comets (JFCs) and Halley-family comets (HFCs). JFCs have short periods of less than 20 years, cross Jupiter's orbit, and are dynamically dominated by major planets (Duncan 2008). HFCs are comets with orbital periods between 20$\sim$200 years and perihelion distances less than 1.5 AU (Bailey & Emel'Yanenko 1996).

To date, there have been many other small bodies which cannot be cataloged into the aforementioned types, such as 1998 WU24 ($e = 0.9$, $q = 1.4$ AU) (Davies et al. 2001) and 1999 LD31 ($e = 0.90$, $q = 2.38$ AU) (Harris et al. 2001), both moving in an eccentric orbit. Both of them share similar orbits with HFCs, without visible signs of outgassing. According to their common properties, these bodies now belong to a new population – the Damocloids (Jewitt 2005).

* Supported by the National Natural Science Foundation of China.

Table 1 Heliocentric ecliptical orbital elements of 2010 EJ104 for TDB epoch 2455400.5 (reference frame is ICRF/J2000).

Element	Value	Uncertainty
a (AU)	21.586266636538866	5.688461074865734E–2
e	0.9011439847926949	2.5546023114618503E–4
i (°)	41.551986960824294	3.1068112777202545E–3
peri (°)	177.04115294493582	7.3861295389317065E–3
node (°)	353.0291168885478	3.357376430876397E–4
t_P (JD)	2455271.4918569964	1.7166562491213885E–2
M (°)	1.2678120987288926	4.901376431292673E–3
q (AU)	2.1339323028906296	1.1173156970862058E–4

The Damocloids are objects which have a Tisserand parameter with respect to Jupiter not larger than two (Jewitt 2005). The Tisserand parameter is expressed as,

$$T_{\rm J} = \frac{a_{\rm J}}{a} + 2\left[(1-e^2)\frac{a}{a_{\rm J}}\right]^{1/2}\cos i, \tag{1}$$

where $a_{\rm J},\ a,\ e$ and i refer to the semi-major axis of Jupiter and the semi-major axis, eccentricity and inclination of the small body, respectively. According to the definition, as of 2011 February, there are 77 Damocloid candidates, consisting of 41 Damocloids with measured decent orbits. The Tisserand parameter is always used to distinguish JFCs from HFCs and other asteroids in the solar system. For JFCs, we have $2 < T_{\rm J} < 3$; but for HFCs we have $T_{\rm J} < 2$, which is also the criterion for Damocloids. However, for other asteroids, one may obtain $T_{\rm J} > 3$.

On 2010 March 10, we discovered a new asteroid moving along a very eccentric orbit, designated as 2010 EJ104. We observed this rapidly moving object using the 1.04/1.20 m Schmidt Telescope (Near Earth Object Survey Telescope) at the Xuyi station of Purple Mountain Observatory (PMO) (Zhao et al. 2008, 2009; Zhao 2010). The orbital elements were then determined by utilizing follow-up measurements from several observatories – the semi-major axis $a = 21.58$ AU, eccentricity $e = 0.90$, inclination $i = 41.55°$, and perihelion distance $q = 2.13$ AU. These orbital elements and their 1 σ uncertainties are shown in Table 1. The orbital features show that this object is similar to 1998 WU24 and 1999 LD31 (Davies et al. 2001; Harris et al. 2001). On the basis of the orbital data, the Tisserand parameter for 2010 EJ104 is about 1.568. Additionally, the object is similar to other members of the Damocloids, which also have no cometary features. Hence, the Damocloids now include a new member, 2010 EJ104, which brings their total number up to 42.

Then a natural question may be raised – where do the Damocloids come from and is there a source or region that may replenish this type of object? Because their orbital properties are similar to those of HFCs, do they arise from the same source, or in other words, are the Damocloids the inactive nuclei of HFCs? Nowadays, several scenarios have been proposed to shed light on possible dynamical origins for such objects.

Firstly, minor objects in the inner solar system can be scattered out due to severe perturbations caused by giant planets (e.g. Jupiter and Neptune) during the secular evolution in the planetesimal's disks (Raymond et al. 2004; Ji et al. 2005, 2011). For example, trans-Neptunian objects can undergo the process of being scattered inward by Neptune (Levison et al. 2009; Moro-Martín 2008). The trans-Neptunian objects are currently postulated to originate from the Kuiper Belt and a scattered disk (Gladman 2005; Morbidelli & Levison 2004). Recently, the dust disk in the Kuiper Belt may have also served as an alternate origin for these objects. Additionally, the region nearby Jupiter may be considered as the birthplace of such objects, where in simulations, $\sim 8\%$ of objects residing in the orbit between Jupiter and 3.3 AU were ejected to an eccentric orbit (Weissman & Levison 1997).

Secondly, there are objects in the outer solar system that could be perturbed by passing massive stars or the tidal effect of the Galactic disk. In the early 1950s, a spherical cloud, consisting of numerous comets ranging from 2000 AU to 50 000 AU, was firstly postulated to mark the distant barrier of the solar system (Oort 1950; Weissman 1990; Dones et al. 2004), which was known as the Oort cloud. Generally speaking, the Sun and major planets play an insignificant part in attracting such bodies due to their great distance. However, the orbital stirrings arising from passing stars or massive planets are quite significant (Morbidelli et al. 2008; Levison et al. 2004) and the tidal effects exerted by the disk (Fouchard et al. 2006) and bulge of the Milky Way may still play a very important part in perturbing these small bodies (Byl 1990). By participating in this complicated dynamical process, the motions of objects in the Oort cloud can be excited and driven into the inner solar system over a longer timescale of evolution.

Recently, an alternative mechanism was proposed to explain the origin of small objects. In this scenario, a hypothetical companion of the Sun (Matese & Whitmire 2011), with a mass of several Jupiters wandering about the innermost region of the outer Oort cloud, may induce the detached Kuiper Belt objects to migrate inward and cross over the disk, then eventually approach the Sun. Consequently, the companion could trigger orbital motions of objects like the Damocloids.

Due to their close similarity, the Damocloids may be inactive nuclei of HFCs (Jewitt 2005; Toth 2006) with the same origin; there are two main sources of HFCs: the scattered disk (Levison et al. 2006) and the inner Oort cloud (Levison et al. 2001) located from 2000 AU to 20 000 AU. Under the gravitational effect of the Sun, eight planets, passing stars, and Galactic tides, with a proper distribution of inclination of about 50°, objects in the inner Oort cloud are stirred up to become HFCs. The scattered disk model may predict that the number of HFCs will be roughly 10 times that of the currently observed results, and the possible outer boundary of the scattered disk is about 200 AU.

In this paper, we extensively study a general origin of the Damocloids through numerical simulations. We find a transient disk located from 700 AU to 1000 AU. Before an object becomes a Damocloid, it may pass through this region. In Section 2, we briefly introduce the method used to numerically investigate the dynamical origin of the Damocloids. Next, we analyze simulation results and discuss the origin mechanisms in Section 3, and we summarize our outcomes in Section 4.

2 METHODS

To better understand the possible dynamical origin of the Damocloids, we investigate their past motion by tracing back the orbits under perturbations from the main planets in the solar system. Backwards integration will illustrate the orbit before the Damocloids moved to the position that we observed. Herein we carry out the backwards numerical simulations in a heliocentric system using a hybrid symplectic algorithm in the MERCURY package (Chambers 1999).

We carry out 29 runs with the 29 target objects shown in Figure 1 from the Damocloid family, including 2010 EJ104. In order to derive the original orbit, we create a swarm of test particles around each target using the nominal orbital element values we observed. The initial semi-major axes, eccentricities and inclinations of the test particles are induced randomly in the range of the element uncertainties. In addition, the other initial orbital elements of each test particle are randomly generated - the arguments of periastron, longitudes of the ascending node, and mean anomalies range from 0° to 360°. For each run, we integrate backwards over a timescale of 10^8 years. Additionally, the parameters of the hybrid integrator are adopted with a stepsize of six days and a Bulirsch-Stoer tolerance of 10^{-12}. In all runs, the gravitational interaction of the Sun and eight major planets in the solar system are fully taken into account during the integration. We stop the calculations when the test particles reach a distance from the central star larger than 1000 AU, which is out of the range of perturbations from the inner solar system (mainly the effect of the eight major planets and the Sun).

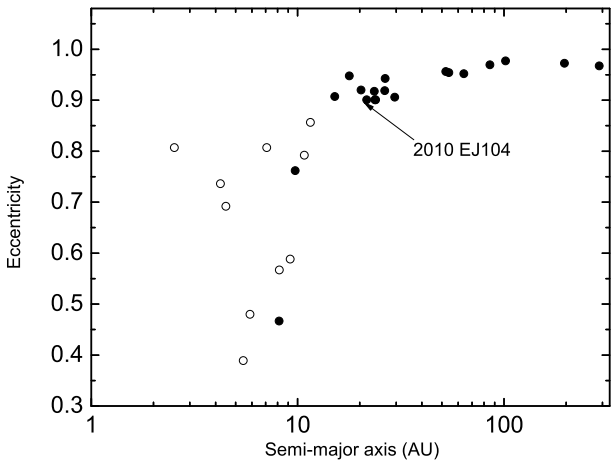

Fig. 1 The semi-major axis versus eccentricity of 29 Damocloids, where 2010 EJ104 is identified out in the figure. According to their possible origin, 29 Damocloids can be classified into two types: types I and II are displayed in solid dots and circles, respectively.

On the other hand, when the test particle approaches a distance closer than the radius of the Sun, we assume that it collides with the Sun.

At the end of the simulation, we record information when one of the conditions is satisfied: I) the orbit of the test particle becomes hyperbolic; II) the distance from the test particle to the Sun is larger than 1000 AU; III) the distance from the test particle to the Sun is closer than the radius of the Sun. The above three conditions are probably caused by the following reasons: I) perturbation from the large planets in the solar system; II) escaping from the inner solar system (here we define $d < 1000$ AU as the inner solar system, d means the distance from the central star); III) having an orbit that glances off the Sun. Thus, by analyzing the record, we will find the possible origin of the Damocloids.

3 THE SCENARIO FOR THE ORIGIN OF DAMOCLOIDS

Now we come to the simulation results. We analyze the results taking 2010 EJ104 as an example.

Figure 2 shows a typical run of 2010 EJ104. In this run, the initial parameters are adopted from Table 1. Eventually, the orbit of this object changes to hyperbolic with a dynamical timescale of ~ 2 Myr at ~ 600 AU, where it may come from.

Figure 3 shows information about the orbit of each test particle for 2010 EJ104 at the end of the simulation. From panel (a) of this figure, it can be noticed that most of the test particles in our simulations mainly return to two regions – the disk at a distance within 300 AU from the Sun (labeled Region I) or a disk between 700 AU and 1000 AU (labeled Region II). Analyzing the results, we find that Region I is mainly composed of two kinds of test particles as shown in panel (b) of Figure 3. One kind is where the orbit becomes hyperbolic at the end of the simulation, and the other is where it collides with the Sun. The test particles in Region II are the ones which almost escaped from the inner solar system with $d > 1000$ AU; the distribution of such test particles is shown in panel (c). Thus, there are two kinds of test particles in Region I. Considering the hyperbolic orbit at the end of the simulation, one part may be involved in the scattering scenario due to stirring by major planets when it lies in the scattered disk (Duncan & Levison 1997) or the Main Belt, especially if

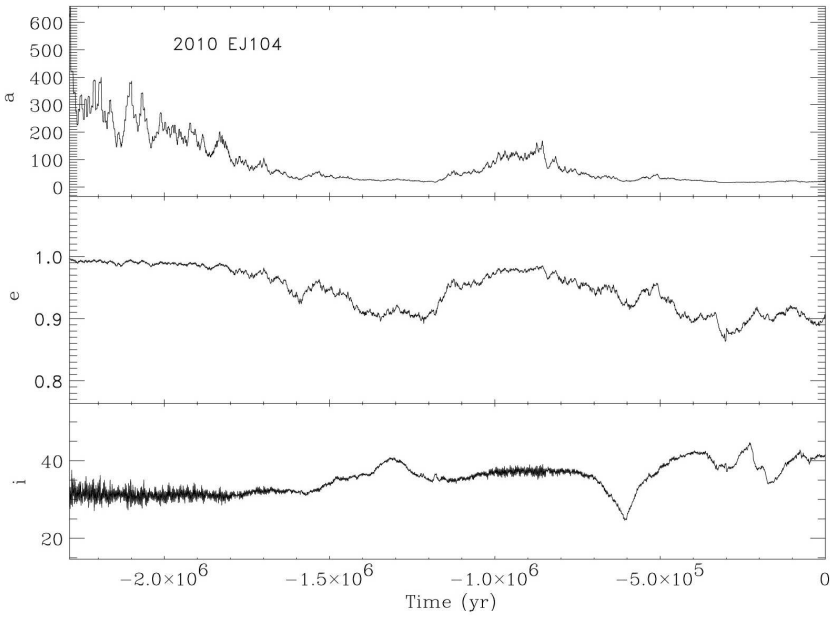

Fig. 2 The orbit of 2010 EJ104 is integrated backwards about 2 Myr. Three panels show the dynamical evolution of its semi-major axis a, eccentricity e, and inclination i, respectively. At the end of the simulation, the object is transferred to a hyperbolic orbit at $\sim$ 600 AU.

the scattered disk encounters Neptune during the dynamical evolution of the solar system (Gladman 2005). The other part represents those that may have originated from glancing off the Sun. In our results, 37% of test particles are in Region I.

The objects in Region II will escape to the outer solar system further than 1000 AU if we continue our calculation. Thus the objects in Region II may be attributed to the Oort cloud by the three mechanisms mentioned above: the first one is the influence of passing stars or massive planets (Morbidelli et al. 2008), the second mechanism is the induced tidal effect by the Galactic disk (Fouchard et al. 2006), and the third scenario may result from the perturbation of the solar companion (Matese & Whitmire 2011). Although the Galactic tides by themselves cannot bring the objects from the inner Oort cloud to the locations within 10^3 AU, about 70% of them with small perihelion can be brought to the inner region of the solar system due to the perturbation of the giant planets (Levison et al. 2001). From the results of Levison et al. (2001), if the object in the inner Oort cloud shows a perihelion distance around the locations of the giant planets in the solar system, gravitational encounters with the giant planets cause a random walk in the semimajor axis. If the semimajor axis decreases to about 30 AU, the giant outer planet will hand it off to the inner giant planet and finally scatter it into the inner solar system. If the semimajor axis increases to a distance larger than 15 000 AU, the effect of the Galactic tide becomes significant and will lead the object to an orbit with a semimajor axis of a few hundred AUs and a small perihelion distance. Another evolutionary process is that a passing star can lower the perihelion distance of the object from the inner Oort cloud to inside Jupiter's orbit. Then the interaction with Jupiter will pull it to the region located from 700 AU to 1000 AU. Figure 13 of their paper shows four kinds of evolutionary processes from the inner Oort cloud to the inner solar system.

Figure 4 in our paper shows the semimajor axes and perihelion distances resulting from all the objects that return to Region II at the end of the simulations. In order to clearly explain our results,

Table 2 Statistical Results of the Damocloids

Name	A	B	C	D	f
2010 NV1	923	77	77	0	0.083
2010 GW147	897	103	103	0	0.115
2004 NN8	891	109	109	0	0.122
2010 JH124	809	191	174	17	0.236
2002 RP120	746	254	245	9	0.340
2000 AB229	731	269	250	19	0.368
2000 HE46	717	283	277	6	0.395
2005 OE	713	287	256	31	0.403
1999 LD31	712	288	280	8	0.404
1997 MD10	695	305	266	39	0.439
2010 OM101	662	338	320	18	0.511
2010 EJ104	630	370	346	24	0.587
2009 YS6	625	375	353	22	0.600
2009 AU16	621	379	344	35	0.610
1998 WU24	601	399	344	55	0.664
2006 RJ2	588	412	390	22	0.701
1999 LE31	573	427	419	8	0.745
1999 XS35	571	429	392	37	0.751
2005 SB223	562	438	389	49	0.779
2000 DG8	427	573	516	57	1.342
2005 TJ50	412	588	513	75	1.427
2004 YH32	387	613	490	123	1.584
2005 NP82	353	647	535	112	1.833
2006 VW266	282	781	557	161	2.546
2009 FW23	243	757	599	158	3.115
2010 LG61	228	772	581	191	3.386
2010 OA101	154	846	541	305	5.494
2007 VA85	126	874	674	200	6.937
2009 HC82	60	940	807	133	15.667

A represents the number of test particles that escaped from the inner solar system; B displays the number of test particles that were perturbed by the main planets or the Sun; C means the number of test particles that were perturbed by the main planets and D means the number of test particles that were perturbed by the Sun. Therefore, $B = C + D$. The value of f is obtained from Eq. (2).

we change our results to a barycentric system in Figures 4 and 5. The perihelion distances shown by the green points in Figure 4 mostly range from 1 AU to 10 AU where they can be perturbed by the main planets. Figure 5 shows a typical evolutionary process. The red line, blue line, and the black line represent the evolution of the semimajor axis, the perihelion distance, and the barycentric distance, respectively. The grey dotted lines display the location of the main planets from Mars to Neptune. The object returns to a barycentric distance of about 10^3 AU. The forthcoming evolutionary process can be described as follows. Firstly, an object from the inner Oort cloud is perturbed to Region II. Then a close encounter with Neptune will hand off the object to Saturn and in turn to Jupiter. Finally, interaction with Jupiter makes it a Damocloid. According to this formation scenario, before an object which comes from the Oort cloud becomes a Damocloid, it must transit the disk. From the statistical result, 63% of test particles return to Region II.

We analyze another 28 groups of simulations and find that the Damocloids mainly return to two regions, as shown in Figure 3. We show our results in Table 2. A represents the number of test particles returning to Region II, while B displays that in Region I. C and D illustrate the number of test particles that are perturbed by the main planets and the Sun, respectively. Thus $B = C + D$ is satisfied. The last column in Table 2 exhibits the ratio of the number in Region I to Region II. In order to clearly illustrate the results, we define three new parameters: f_{RegionI} to f_{RegionII} mean the

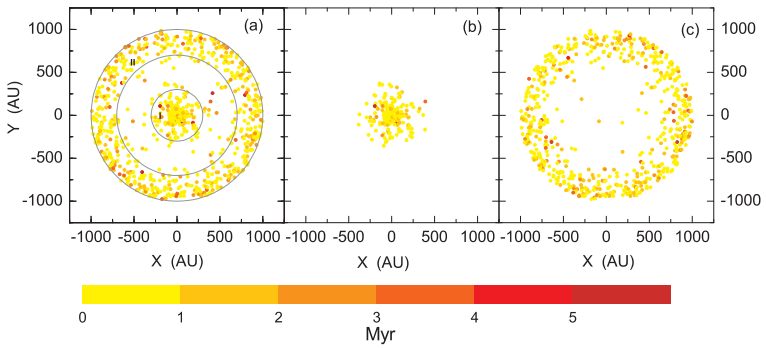

Fig. 3 Results of backward simulations. Based on observational uncertainties, all test bodies are initially set to be 21.586 $\pm$ 0.057 AU. In the figure, all bodies had been tracked to find their birthplace. The bodies from the disk within 300 AU are marked as Region I (inside the innermost circle), while those from 700 $\sim$ 1000 AU are labeled Region II (the outer belt). The average lifetime of all bodies is about 9.93×10^5 years, where a deeper color index indicates a longer lifetime. Panel (b) shows the test particles whose orbits became hyperbolic or collided with the Sun. Panel (c) shows the test particles which escaped from the inner solar system.

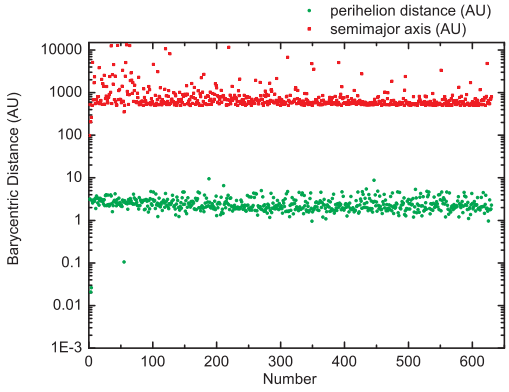

Fig. 4 Statistical results of the objects which return to Region II in the simulation of 2010 EJ104. The red filled squares are the semimajor axes and the green points represent the perihelion distances.

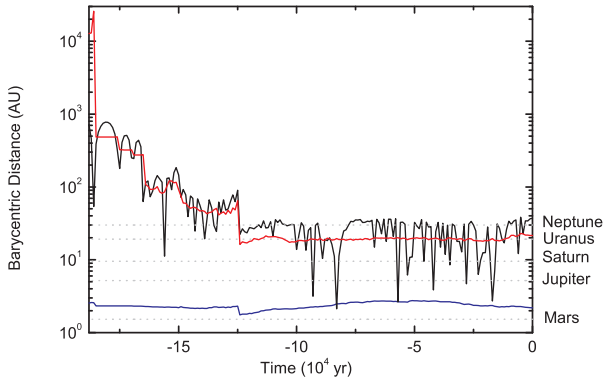

Fig. 5 Typical result of the object which returns to Region II. The red line indicates the evolution of the semimajor axis, the blue line represents the perihelion distance and the black line shows the evolution of the barycentric distance. The grey dotted lines display the location of the main planets from Mars to Neptune.

probability of the Damocloids coming from Regions I or II, respectively, and f is expressed as

$$f = \frac{f_{\rm RegionI}}{f_{\rm RegionII}}. \quad (2)$$

From the results in Table 2 and the definition of f, the Damocloids can be further categorized into two types.

(1) Type I: $f < 1$. Similar to the case of 2010 EJ104, over 50% of the test particles return to Region II. This means that the perturbation from the Oort cloud is the main reason for the formation of this type of Damocloid. In this case, 19 of 29 Damocloids can be grouped into Type I, which are labeled as solid dots in Figure 1.
(2) Type II: $f > 1$. Different from type I, a perturbation in the inner solar system, including the effect of the eight major planets and the Sun, leads to the formation of Damocloids. However, the scattered disk may be the most probable origin of the Damocloids. Ten Damocloids in our samples are this type, which are marked as circles in Figure 1.

From the distribution of dots in Figure 1, we notice that Types I and II have apparently defined a boundary at about 15 AU. Based on the statistical results for 29 Damocloid, the average probability of the Damocloid population originating from Regions I or II is about 34.5% and 65.5%, respectively.

As mentioned in the first section, HFCs mainly come from two possible regions, the scattered disk or the inner Oort cloud. According to our results, the Damocloids can also come from two regions, the scattered disk or the Oort cloud, which will be perturbed into the transient disk located from 700 AU to 1000 AU. In this sense, the same origin could imply that Damocloids are the inactive nuclei of HFCs. In the future, following a more careful investigation, we will obtain more detailed results.

4 CONCLUSIONS AND DISCUSSION

On the basis of the overall dynamical analysis, we underline that two regions are likely to serve as the birthplace for the Damocloids, the scattered disk inside 100 AU (corresponding to Region I) and the Oort cloud (corresponding to Region II). According to their possible origin, they can be further classified into two types: type I indicates that the objects mainly come from the Oort cloud, which corresponds to the backward orbit to Region II; type II suggests that the population mostly comes from the scattered disk, which will be perturbed by the major planets or the Sun.

In this work, we did not consider the effect of the outer solar system. Thus, evolution in a region with a distance from the central star larger than 1000 AU is not clear. If the Damocloids come from the inner Oort cloud, we may briefly summarize the possible routes for such objects: firstly, the bodies in the Oort cloud could be stirred by perturbations from passing stars or the tidal effect of the Galactic disk, then fall inward to the intermediate region (Region II), and finally injected to the inner solar system.

Additionally, the outer asteroid belt is another possible origin of Damocloids. Bodies removed from this region are found to fall under the gravitational influence of Jupiter, which scatters them to large heliocentric distances (Fernández et al. 2002). It is then possible that some scattered asteroids can return as Damocloids.

In this paper, we only study the origin of Damocloids from the point of view of backward simulations. Thus, the scattered disk and the inner Oort cloud are just two possible origins of Damocloids. However, there are still other possible origins, such as the asteroid belt including the main belt and the outer belt. As more members of Damocloids are observed in the future, their origin can be better explained.

Acknowledgements We thank Zhaori Getu, Hong Renquan and Hu Longfei who have greatly contributed to observations of the asteroid survey. Wang S. is supported by the National Natural Science Foundation of China (Grant Nos. 10925313 and 10833001) and the China Postdoctoral Science Foundation (Grant No. 2011M500962). Z.H.B is supported by the National Natural Science Foundation of China (Grant Nos. 10503013 and 10933004). J.J.H is grateful for support by the National Natural Science Foundation of China (Grant Nos. 11273068, 10973044 and 10833001), the Natural Science Foundation of Jiangsu Province (Grant No. BK2009341), the Foundation of Minor Planets of Purple Mountain Observatory, and the innovative and interdisciplinary program by CAS (Grant No. KJZD-EW-Z001).

References

Bailey, M. E., & Emel'Yanenko, V. V. 1996, MNRAS, 278, 1087
Byl, J. 1990, AJ, 99, 1632
Chambers, J. E. 1999, MNRAS, 304, 793
Davies, J. K., Tholen, D. J., Whiteley, R. J., et al. 2001, Icarus, 150, 69
Dones, L., Weissman, P. R., Levison, H. F., & Duncan, M. J. 2004, in Comets II, Oort Cloud Formation and Dynamics, eds. M. C. Festou, H. U. Keller, & H. A. Weaver (Tucson: Univ. Arizona), 153
Duncan, M. J. 2008, Space Sci. Rev., 138, 109
Duncan, M. J., & Levison, H. F. 1997, Science, 276, 1670
Fernández, J. A., Gallardo, T., & Brunini, A. 2002, Icarus, 159, 358
Fouchard, M., Froeschlé, C., Valsecchi, G., & Rickman, H. 2006, Celestial Mechanics and Dynamical Astronomy, 95, 299
Gladman, B. 2005, Science, 307, 71
Harris, A. W., Delbó, M., Binzel, R. P., et al. 2001, Icarus, 153, 332
Jewitt, D. 2005, AJ, 129, 530
Ji, J., Liu, L., Kinoshita, H., & Li, G. 2005, ApJ, 631, 1191
Ji, J., Jin, S., & Tinney, C. G. 2011, ApJ, 727, L5
Levison, H. F., Dones, L., & Duncan, M. J. 2001, AJ, 121, 2253
Levison, H. F., Morbidelli, A., & Dones, L. 2004, AJ, 128, 2553
Levison, H. F., Duncan, M. J., Dones, L., & Gladman, B. J. 2006, Icarus, 184, 619
Levison, H. F., Bottke, W. F., Gounelle, M., et al. 2009, Nature, 460, 364
Matese, J. J., & Whitmire, D. P. 2011, Icarus, 211, 926
Morbidelli, A., & Levison, H. F. 2004, AJ, 128, 2564
Morbidelli, A., Levison, H. F., & Gomes, R. 2008, in The Solar System Beyond Neptune, The Dynamical Structure of the Kuiper Belt and Its Primordial Origin, 275
Moro-Martín, A. 2008, in IAU Symposium, 249, eds. Y.-S. Sun, S. Ferraz-Mello, & J.-L. Zhou, 347
Oort, J. H. 1950, Bull. Astron. Inst. Netherlands, 11, 91
Raymond, S. N., Quinn, T., & Lunine, J. I. 2004, Icarus, 168, 1
Toth, I. 2006, in Asteroids, Comets, Meteors, IAU Symposium, 229, eds. L. Daniela, M. Sylvio Ferraz, & F. J. Angel, 67
Weissman, P. R. 1990, Nature, 344, 825
Weissman, P. R., & Levison, H. F. 1997, ApJ, 488, L133
Zhao, H. B., Yao, J. S., & Lu, H. 2008, in IAU Symposium, 248, eds. W. J. Jin, I. Platais, & M. A. C. Perryman, 565
Zhao, H., Lu, H., Zhaori, G., Yao, J., & Ma, Y. 2009, Science in China G: Physics and Astronomy, 52, 1790
Zhao, H. B. 2010, Acta Astronomica Sinica, 51, 324